

Gluonic Tetracharm Configuration of $X(6900)$

Bing-Dong Wan¹ and Cong-Feng Qiao^{1,2*}

¹ *School of Physics, University of Chinese Academy
of Science, Yuquan Road 19A, Beijing 10049*

² *CAS Center for Excellence in Particle Physics, Beijing 10049, China*

Abstract

Recently, a new hadronic structure around 6.9 GeV was observed in LHCb experiment. From its limited yet known decay mode, one may still figure out that it contains at least four charm quarks and hence belongs to the category of exotic state. This finding activates the door into double hidden charm exotic states, and hence has a peculiar importance. In this letter we propose a nature hybrid interpretation for the structure of $X(6900)$, i.e. in $[3_c]_{cc} \otimes [8_c]_G \otimes [3_c]_{\bar{c}\bar{c}}$ configuration with $J^{PC} = 0^{++}$, and by virtue of the QCD Sum Rule technique we perform the mass spectrum calculation. The results suggest our conjecture and more pending detecting structures, e.g. the one around 7.2 GeV in the double hidden-charm hybrid configuration and with $J^{PC} = 0^{-+}$. We predict also the hidden quobottom hybrid states, leaving for experimental confirmation.

* qiaocf@ucas.ac.cn

The establishment of quark model (QM) in the 50s of last century is a milestone in the pilgrimage to micro world [1, 2]. The spectroscopy of conventional meson and baryon in QM are as of yet gradually confirmed in experiment and are going to be complete. Entering the new millennium, with the development of technology the so-called exotic state emerges in experiment, like $X(3872)$ [3], and new ones tend to appear more frequently. Now we already have a bunch of exotic candidates waiting for characterizing, similar to the phase of "particle zoo" in last century. To discover more exotic states and explore their properties are one of the most intriguing and important topics in particle physics for nowadays physicists, which may promote our understanding of quantum chromodynamics (QCD) and enrich our knowledge of hadron spectroscopy.

In light hadron sector, because normally the spacings between various states are small, it is tough to split the exotic states from the conventional hadrons, except the former possess some peculiar quantum numbers. In contrast, the exotic states in heavy hadron sector may have relatively distinct signatures. Indeed, in recent years a bunch of so-called plethora charmonium-/bottomonium-like states XYZ are observed in experiment [3–7], which provides a new horizon for our understanding of the emergence of structures in quantum chromodynamics (QCD).

Recently, using proton-proton collision data at centre-of-mass energies of $\sqrt{s} = 7, 8$ and 13 TeV, LHCb Collaboration observed a narrow structure in J/ψ -pair invariant mass of about 6.9 GeV with the significance greater than 5σ [8]. In addition to the narrow $X(6900)$, a broad structure just above double J/ψ threshold ranging and one around 7.2 GeV were also reported. This is the first time that clear structures in the J/ψ -pair mass spectrum have been observed experimentally and if it is further confirmed to be a hadronic structure, rather than the kinematic effect, it turns out to be a remarkable discovery in the exploration of hadron spectroscopy, the novel double hidden-charm state.

About double hidden-charm(bottom) states there have been some investigations in the literature [9–28], and most of these theoretical studies fall in the experimental measurement about the broad structure [8]. However, the narrow structure $X(6900)$ is higher than double J/ψ threshold by 700 MeV or so, much larger than the typical energy gap between ground and excited states. Instead of attributing $X(6900)$ as a naive four-quark state via certain fancy

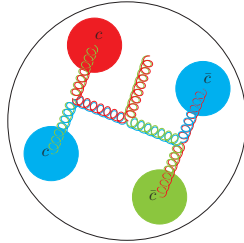


FIG. 1: A cartoon of double hidden-charm hybrid.

mechanisms, we suggest this structure be a double hidden-charm hybrid, which contains a pair of constituent diquarks and a dynamic gluon, as shown in Fig. 1.

Within the double hidden-charm hybrid model, the $c(\bar{c}) - c(\bar{c})$ composes a relatively compact diquark state in representation $\bar{3}$ of SU(3) gauge group, which was once employed to interpret the pentaquark state $\Theta(1540)$ [29]. Hybrid is a kind of hadronic structure, which is accessible in light of QCD formalism, while has still no clear evidence in experiment. The hybrid charmonium model was applied to explain the $Y(4260)$ [30], a somehow established exotic state.

We evaluate the four-quark hybrid by virtue of the model independent Shifman, Vainshtein and Zakharov (SVZ) QCD sum rule technique [31]. The SVZ sum rule, viz QCD sum rule, has some peculiar advantages in exploring hadron properties involving nonperturbative QCD. It is a QCD based theoretical framework which incorporates nonperturbative effects universally order by order, rather a phenomenological model, and has already achieved a lot in the study of hadron spectroscopy and decays. To establish the sum rules, the starting point is to construct the proper interpolating currents corresponding to the hadron of interest. Then, roughly, by matching operator product expansion (OPE) to the hadronic saturation to establish sum rules capable of extracting the hadron mass or decay rate.

In this work, aiming at understanding the nature of $X(6900)$, we investigate the double hidden-charm hybrid in QCD sum rule with composite current quantum numbers of $J^P = 0^{++}$ and 0^{-+} , which exhibit to be the simplest ones. Their bottom partner are also evaluated by a similar way.

The lowest order possible interpolating currents of 0^{++} and 0^{-+} double hidden-charm

hybrid states take the following forms:

$$j_{0^{A}++}^A(x) = g_s \epsilon_{ikl} \epsilon_{jmn} [c_k^T C \gamma_\mu c_l] \frac{\lambda_{ij}^a}{2} G_{\mu\nu}^a [\bar{c}_m \gamma_\nu C \bar{c}_n^T], \quad (1)$$

$$j_{0^{B}++}^B(x) = g_s \epsilon_{ikl} \epsilon_{jmn} [c_k^T C \gamma_\mu \gamma_5 c_l] \frac{\lambda_{ij}^a}{2} G_{\mu\nu}^a [\bar{c}_m \gamma_\nu \gamma_5 C \bar{c}_n^T], \quad (2)$$

$$j_{0^{-}+}^A(x) = g_s \epsilon_{ikl} \epsilon_{jmn} [c_k^T C \gamma_\mu c_l] \frac{\lambda_{ij}^a}{2} \tilde{G}_{\mu\nu}^a [\bar{c}_m \gamma_\nu C \bar{c}_n^T], \quad (3)$$

$$j_{0^{-}+}^B(x) = g_s \epsilon_{ikl} \epsilon_{jmn} [c_k^T C \gamma_\mu \gamma_5 c_l] \frac{\lambda_{ij}^a}{2} \tilde{G}_{\mu\nu}^a [\bar{c}_m \gamma_\nu \gamma_5 C \bar{c}_n^T], \quad (4)$$

where g_s is the strong coupling constant, i, j, k, \dots are color indices, μ and ν are Lorentz indices, λ^a are the Gell-Mann matrices, and C represents the charge conjugation matrix. Here, $G_{\mu\nu}^a$ is the gluon field strength and $\tilde{G}_{\mu\nu}^a = \epsilon_{\mu\nu\alpha\beta} G^{\alpha\beta}$ denotes its dual field strength.

With the currents (1)–(4), the two-point correlation function can be readily established, i.e.,

$$\Pi_{J^{PC}}^k(q^2) = i \int d^4x e^{iq \cdot x} \langle 0 | T \{ j_{J^{PC}}^k(x), j_{J^{PC}}^k(0)^\dagger \} | 0 \rangle, \quad (5)$$

where the subscript J^{PC} denotes the quantum number of the involved hybrid state, k runs from A to B , and $|0\rangle$ denotes the physical vacuum. The Feynman diagrams of the correlation function in calculation are shown in Fig. 2.

In the partonic representation, the dispersion relation may express the correlation function $\Pi_{J^{PC}}^k$ as

$$\Pi_{J^{PC}}^{k, OPE}(q^2) = \int_{s_{min}}^{\infty} ds \frac{\rho_{J^{PC}}^{k, OPE}(s)}{s - q^2}. \quad (6)$$

Here, $\rho_{J^{PC}}^{k, OPE}(s) = \text{Im}[\Pi_{J^{PC}}^{k, OPE}(s)]/\pi$ and s_{min} is a kinematic limit, which usually corresponds to the square of the sum of the current quark masses of the hadron [32], i.e., $s_{min} = 16m_c^2$.

By applying the Borel transformation to (6), we then have

$$\Pi_{J^{PC}}^{k, OPE} = \int_{s_{min}}^{\infty} ds \rho_{J^{PC}}^{k, OPE}(s) e^{-s/M_B^2}. \quad (7)$$

In the hadronic representation, after isolating the ground state contribution from the hadronic state, we obtain the correlation function $\Pi_{J^{PC}}^k(q^2)$ in dispersion integral over the physical region, i.e.,

$$\Pi_{J^{PC}}^{k, phen}(q^2) = \frac{(\lambda_{J^{PC}}^k)^2}{(m_{J^{PC}}^k)^2 - q^2} + \frac{1}{\pi} \int_{s_0}^{\infty} ds \frac{\rho_{J^{PC}}^k(s)}{s - q^2}, \quad (8)$$

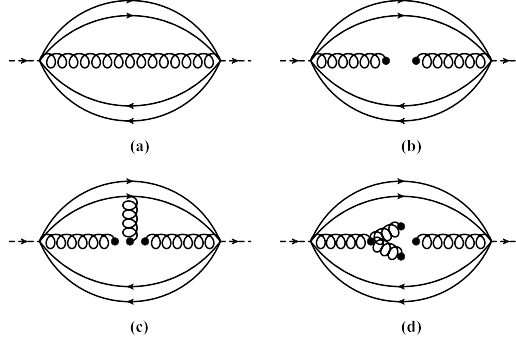


FIG. 2: The typical Feynman diagrams of the double hidden-charm hybrid, where the permutation diagrams are implied. Here, (a), (b), (c), and (d) represent respectively the contributions from perturbative, two-gluon condensate, and tri-gluon condensates.

where m_{JPC}^k denotes the mass of the lowest lying hybrid state, $\rho_{JPC}^k(s)$ is the spectral density that contains the contributions from higher excited states, λ_{JPC}^k is the coupling constant and the continuum states above the threshold s_0 .

By performing the Borel transform on the hadronic side, Eq.(8), and matching it to Eq.(7), we can then obtain the mass of the double hidden-charm hybrid state,

$$m_{JPC}^k(s_0, M_B^2) = \sqrt{-\frac{L_{JPC,1}^k(s_0, M_B^2)}{L_{JPC,0}^k(s_0, M_B^2)}}. \quad (9)$$

Here the moments L_1 and L_0 are defined as:

$$L_{JPC,0}^k(s_0, M_B^2) = \int_{s_{min}}^{s_0} ds \rho_{JPC}^{k,OPE}(s) e^{-s/M_B^2}, \quad (10)$$

$$L_{JPC,1}^k(s_0, M_B^2) = \frac{\partial}{\partial \frac{1}{M_B^2}} L_{JPC}^{k,OPE}(s_0, M_B^2). \quad (11)$$

In the numerical calculation, the input parameters we take are [31–35]: $m_c(m_c) = \overline{m}_c = (1.275 \pm 0.025)$ GeV, $m_b(m_b) = \overline{m}_b = (4.18 \pm 0.03)$ GeV, $\langle g_s^2 G^2 \rangle = 0.88$ GeV⁴, $\langle g_s^3 G^3 \rangle = 0.045$ GeV⁶, in which the $\overline{\text{MS}}$ running heavy quark masses are adopted. Furthermore, the leading order strong coupling constant

$$\alpha_s(M_B^2) = \frac{4\pi}{(11 - \frac{2}{3}n_f) \ln(\frac{M_B^2}{\Lambda_{\text{QCD}}^2})} \quad (12)$$

with $\Lambda_{\text{QCD}} = 300$ MeV is taken, and n_f , here 5, stands for the number of active quarks.

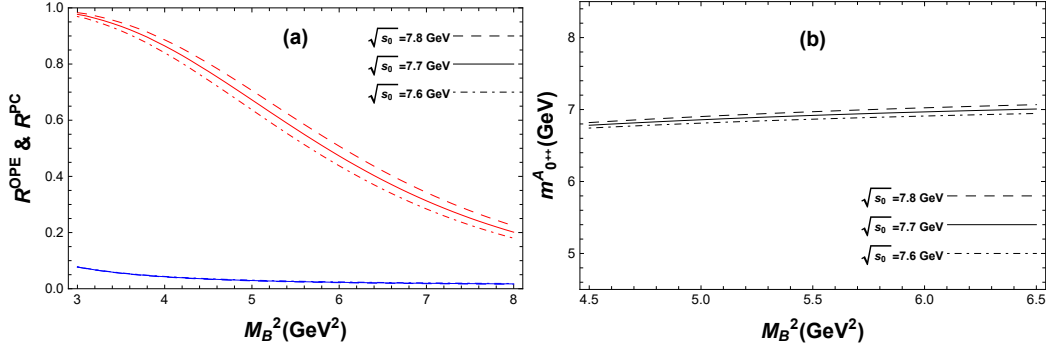


FIG. 3: (a) The ratios $R_{0^{++}}^{A, OPE}$ and $R_{0^{++}}^{A, PC}$ as functions of the Borel parameter M_B^2 for different values of $\sqrt{s_0}$, where blue lines represent $R_{0^{++}}^{A, OPE}$ and red lines denote $R_{0^{++}}^{A, PC}$. (b) The mass $M_{0^{++}}^A$ as a function of the Borel parameter M_B^2 for different values of $\sqrt{s_0}$.

Moreover, there exist two additional parameters M_B^2 and s_0 introduced in establishing the sum rules, which will be fixed in light of the so-called standard procedures abiding by two criteria [31–34]. The first one asks for the convergence of the OPE. That is, one needs to compare individual contributions with the total magnitude on the OPE side, and choose a reliable region for M_B^2 to retain the convergence. The second criterion requires that the portion of lowest lying pole contribution (PC), the ground state contribution, in the total, pole plus continuum, should be over 50% [36, 37]. The two criteria can be formulated as

$$R_{JPC}^{k, OPE} = \left| \frac{L_{JPC, 0}^{k, \langle g_s^3 G^3 \rangle}(s_0, M_B^2)}{L_{JPC, 0}^k(s_0, M_B^2)} \right|, \quad (13)$$

$$R_{JPC}^{k, PC} = \frac{L_{JPC, 0}^k(s_0, M_B^2)}{L_{JPC, 0}^k(\infty, M_B^2)}. \quad (14)$$

In order to find a proper value for continuum threshold s_0 , we perform a similar analysis as in Refs. [36, 37]. Therein, one needs to find out the proper value, which has an optimal window for the mass curve of the interested hadron. Within this window, the physical quantity, that is the mass of the concerned hadron, is independent of the Borel parameter M_B^2 as much as possible. In practice, we may vary $\sqrt{s_0}$ by 0.1 GeV in numerical calculation [36, 37], which sets the upper and lower bounds and hence the uncertainties of $\sqrt{s_0}$.

With above preparation we numerically evaluate the mass spectrum of the double hidden-charm hybrid states. For the current in Eq. (1), the ratios $R_{0^{++}}^{A, OPE}$ and $R_{0^{++}}^{A, PC}$ are shown

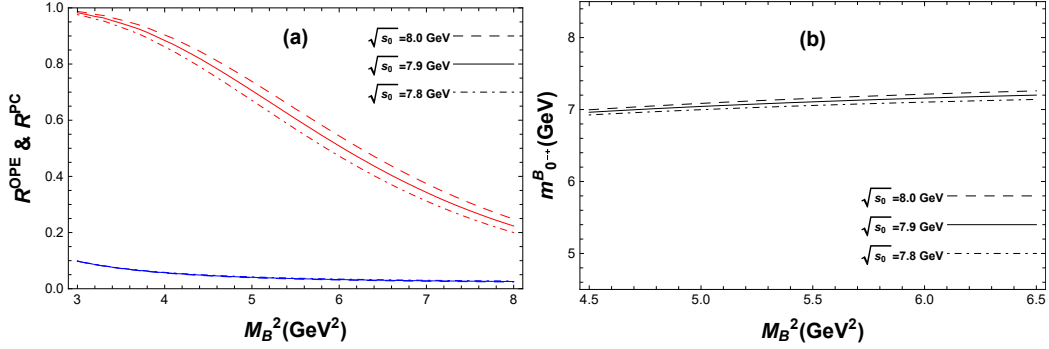


FIG. 4: The same caption as in Fig 3, but for the $R_{0^{++}}^{B, OPE}$, $R_{0^{++}}^{B, PC}$, and $M_{0^{++}}^B$.

as functions of Borel parameter M_B^2 in Fig. 3(a) with different values of $\sqrt{s_0}$, i.e. 7.6, 7.7, and 7.8 GeV. The dependency relations between $m_{0^{++}}^A$ and parameter M_B^2 are given in Fig. 3(b). The optimal window of Borel parameter sits in between $4.8 \leq M_B^2 \leq 5.9$ GeV², where a smooth section, the so called stable plateau, in the $m_{0^{++}}^A - M_B^2$ curve exists, suggesting the mass of the possible 0^{++} double hidden-charm hybrid state. Then the mass $m_{0^{++}}^A$ can be extracted as

$$m_{0^{++}}^A = (6.92 \pm 0.14) \text{ GeV} . \quad (15)$$

This mass value is in good agreement with the observed mass of the $X(6900)$ state [8], and implies a possible $J^{PC} = 0^{++}$ double hidden-charm hybrid interpretation.

For the currents in Eqs. (2) and (3), we can not obtain positive spectral density functions $\rho_{0^{++}}^B$ and $\rho_{0^{+-}}^A$, which means the current structures in Eqs. (2) and (3) do not support the corresponding hybrid states.

For the current (4), the ratios $R_{0^{+-}}^{B, OPE}$ and $R_{0^{+-}}^{B, PC}$ are shown as functions of Borel parameter M_B^2 in Fig. 4(a) with different values of $\sqrt{s_0}$ as well, and the dependency relations between $m_{0^{+-}}^B$ and parameter M_B^2 are given in Fig. 4(b). The optimal window for Borel parameter is found in between $4.9 \leq M_B^2 \leq 6.0$ GeV², where a stable plateau in the $m_{0^{+-}}^B - M_B^2$ curve emerges, suggesting the mass of a possible 0^{+-} double hidden-charm hybrid state as

$$m_{0^{+-}}^B = (7.10 \pm 0.12) \text{ GeV} . \quad (16)$$

This mass fits well with the signature of the recent observation around 7.2 GeV [8].

In the results (15) and (16), uncertainties stem from the uncertainties of the quark masses, the Borel parameter M_B^2 and the threshold parameter $\sqrt{s_0}$.

In analogous, we may evaluate the double hidden-bottom hybrid states. Employing the obtained analytical results but with m_c being replaced by m_b , the masses of the double hidden-bottom hybrid states are readily obtained, that is

$$m_{0^{++}}^{A,b} = (19.30 \pm 0.23) \text{ GeV} , \quad (17)$$

$$m_{0^{-+}}^{B,b} = (19.46 \pm 0.20) \text{ GeV} . \quad (18)$$

Here, the superscript b denotes the b -sector hybrid.

In summary, a novel double hidden-charm hybrid configuration, i.e. $[3_c]_{cc} \otimes [8_c]_G \otimes [3_c]_{\bar{c}\bar{c}}$, is proposed to interpret the hadronic structure $X(6900)$ recently observed in LHCb experiment. In this picture, we explore the hybrid states with quantum numbers $J^{PC} = 0^{++}$ and 0^{-+} , the lowest energy states, in the frame work of QCD sum rule. Two stable hybrid states are obtained with masses about 6.92 and 7.10 GeV for $J^{PC} = 0^{++}$ and 0^{-+} , respectively, which fit well to experimental measurements within the error of uncertainties. Moreover, their b -sector partners are also evaluated, and find two states with masses (19.30 ± 0.23) and (19.46 ± 0.20) GeV for 0^{++} and 0^{-+} , respectively.

Last, it should be noted that although it was argued by Czarnecki *et al.* [38] that due the nonexistence of two strongly separated mass scales, stable tetrons, such as a double bottomonium $b\bar{b}\bar{b}$ or double charmonium $c\bar{c}\bar{c}$ system, may not exist, the double hidden-charm and -bottom hybrids are in different situation. One straightforward experimental veto on our model and others would be the measurement on $J/\psi \psi'$ or double ψ' invariant mass.

Acknowledgments

This work was supported in part by the National Natural Science Foundation of China(NSFC) under the Grants 11975236 and 11635009.

[1] M. Gell-Mann, Phys. Lett. **8**, 214 (1964).

[2] G. Zweig, Report No. CERN-TH-401.

- [3] S. K. Choi *et al.* [Belle Collaboration], Phys. Rev. Lett. **91**, 262001 (2003).
- [4] B. Aubert *et al.* [BaBar Collaboration], Phys. Rev. Lett. **95**, 142001 (2005).
- [5] A. Bondar *et al.* [Belle Collaboration], Phys. Rev. Lett. **108**, 122001 (2012).
- [6] M. Ablikim *et al.* [BESIII Collaboration], Phys. Rev. Lett. **110**, 252001 (2013).
- [7] Z. Q. Liu *et al.* [Belle Collaboration], Phys. Rev. Lett. **110**, 252002 (2013).
- [8] R. Aaij *et al.* [LHCb], Sci. Bull. **65**, 1983 (2020).
- [9] Y. Iwasaki, Phys. Rev. Lett. **36**, 1266 (1976).
- [10] K. T. Chao, Z. Phys. **C7**, 317 (1981).
- [11] J. P. Ader, J. M. Richard and P. Taxil, Phys. Rev. **D25**, 2370 (1982).
- [12] M. Karliner, S. Nussinov and J. L. Rosner, Phys. Rev. **D95**, 034011 (2017).
- [13] N. Barnea, J. Vijande and A. Valcarce, Phys. Rev. **D73**, 054004 (2006).
- [14] V. R. Debastiani and F. S. Navarra, Chin. Phys. **C43**, 013105 (2019).
- [15] M. S. Liu, Q. F. Lü, X. H. Zhong and Q. Zhao, Phys. Rev. **D100**, 016006 (2019).
- [16] W. Chen, H. X. Chen, X. Liu, T. G. Steele and S. L. Zhu, Phys. Lett. **B773**, 247(2017).
- [17] G. J. Wang, L. Meng and S. L. Zhu, Phys. Rev. **D100**, 096013 (2019).
- [18] R. J. Lloyd and J. P. Vary, Phys. Rev. **D70**, 014009 (2004).
- [19] M. N. Anwar, J. Ferretti, F. K. Guo, E. Santopinto and B. S. Zou, Eur. Phys. J. **C78**, 647 (2018).
- [20] Z. G. Wang, Eur. Phys. J. **C77**, 432 (2017).
- [21] X. Jin, Y. Xue, H. Huang and J. Ping, [arXiv:2006.13745 [hep-ph]].
- [22] Q. F. Lü, D. Y. Chen and Y. B. Dong, Eur. Phys. J. **C80**, 871 (2020).
- [23] G. Yang, J. Ping, L. He and Q. Wang, [arXiv:2006.13756 [hep-ph]].
- [24] Z. G. Wang, Chin. Phys. **C44**, 113106 (2020).
- [25] R. M. Albuquerque, S. Narison, A. Rabemananjara, D. Rabetiarivony and G. Randriamanatrika, Phys. Rev. **D102**, 094001 (2020).
- [26] J. Sonnenschein and D. Weissman, [arXiv:2008.01095 [hep-ph]].
- [27] J. F. Giron and R. F. Lebed, Phys. Rev. **D102**, 074003 (2020).
- [28] M. S. liu, F. X. Liu, X. H. Zhong and Q. Zhao, [arXiv:2006.11952 [hep-ph]].
- [29] R. Jaffe and F. Wilczek, Phys. Rev. Lett. **91**, 232003 (2003).
- [30] F.E. Close and P.R. Page, Phys. Lett. **B628**, 215 (2005).
- [31] M.A. Shifman, A.I. Vainshtein and V.I. Zakharov, Nucl. Phys. **B147**, 385 (1979); *ibid*, Nucl. Phys. **B147**, 448 (1979).
- [32] R. M. Albuquerque, arXiv:1306.4671 [hep-ph].
- [33] L. J. Reinders, H. Rubinstein and S. Yazaki, Phys. Rept. **127**, 1 (1985).
- [34] P. Colangelo and A. Khodjamirian, in *At the frontier of particle physics / Handbook of QCD*, edited by M. Shifman (World Scientific, Singapore, 2001), arXiv:hep-ph/0010175.

- [35] S. Narison, World Sci. Lect. Notes Phys. **26** 1 (1989) .
- [36] C. F. Qiao and L. Tang, Phys. Rev. Lett. **113**, 221601 (2014).
- [37] L. Tang and C. F. Qiao, Nucl. Phys. **B904**, 282 (2016).
- [38] Andrzej Czarnecki, Bo Leng, and M.B. Voloshin, Phys. Lett. **B778**, 233 (2018).

Appendix A: The spectral densities of Z_{cs}^+

In order to calculate the spectral density of the operator product expansion (OPE) side, the heavy-quark ($Q = c$ or b) full propagator $S_{ij}^Q(p)$ is employed, say

$$S_{jk}^Q(p) = \frac{i\delta_{jk}(\not{p} + m_Q)}{p^2 - m_Q^2} - \frac{i}{4} \frac{t_{jk}^\alpha G_{\alpha\beta}^a}{(p^2 - m_Q^2)^2} [\sigma^{\alpha\beta}(\not{p} + m_Q) + (\not{p} + m_Q)\sigma^{\alpha\beta}]. \quad (\text{A1})$$

Here, the vacuum condensates are explicitly shown. For more explanation on above propagators, readers may refer to Refs. [32]. In the partonic representation, spectral density may be expressed as:

$$\rho^{OPE}(s) = \rho^{pert}(s) + \rho^{\langle G^2 \rangle}(s) + \rho^{\langle G^3 \rangle}(s). \quad (\text{A2})$$

1. The spectral densities for 0^{++} double hidden-charm hybrid

The spectral density $\rho^{OPE}(s)$ is calculated up to dimension six. For all currents showed in Eqs. (1) and (2), we obtain the spectral densities as follows:

$$\begin{aligned} \rho_i^{pert}(s) &= \frac{g_s^2}{2^{10} \times 5 \times \pi^8} \int_{x_-}^{x_+} dx \int_{y_-}^{y_+} dy \int_{z_-}^{z_+} dz \int_{w_-}^{w_+} dw A_{xyzw} H_{xyzw}^3 \\ &\times \left\{ 4A_{xyzw} H_{xyzw}^3 xyzw - 2H_{xyzw}^2 [18xyzw A_{xyzw} s + \mathcal{N}_i(xy + zw)m_c^2] \right. \\ &+ 20A_{xyzw}(m_c^4 - xyzws^2) + 5H_{xyzw} [12xyzw A_{xyzw} s^2 \\ &+ \mathcal{N}_i(xy + zw)m_c^2 s + 2(A_{xyzw} - 1)m_c^4] \left. \right\}, \quad (\text{A3}) \end{aligned}$$

$$\begin{aligned} \rho_i^{\langle G^2 \rangle}(s) &= \frac{\langle g_s^2 G^2 \rangle}{2^9 \times 3 \times \pi^6} \int_{x_-}^{x_+} dx \int_{y_-}^{y_+} dy \int_{z_-}^{z_+} dz F_{xyz}^2 \\ &\times \left\{ 6m_c^4 + \mathcal{N}_i m_c^2 (3s - 2F_{xyz})(xy + zB_{xyz}) \right\}, \quad (\text{A4}) \end{aligned}$$

$$\begin{aligned} \rho_i^{\langle G^3 \rangle}(s) &= \frac{\langle g_s^3 G^3 \rangle}{2^8 \times \pi^6} \int_{x_-}^{x_+} dx \int_{y_-}^{y_+} dy \int_{z_-}^{z_+} dz \left\{ \frac{1}{2} [4xyz B_{xyz} F_{xyz}^3 \right. \\ &- s(m_c^2 + \mathcal{N}_i xys)(m_c^2 + \mathcal{N}_i zs B_{xyz}) - 3F_{xyz}^2 (6sxyz B_{xyz} + \mathcal{N}_i m_c^2 (xy + zB_{xyz})) \\ &+ 2F_{xyz} (m_c^4 + 6s^2 xyz B_{xyz} + 3\mathcal{N}_i s m_c^2 (xy + zB_{xyz})) \\ &\left. + \frac{m_c^2 F_{xyz}}{x} [\mathcal{N}_i (F_{xyz} - s)(xy + zB_{xyz}) - 2m_c^2] \right\}, \quad (\text{A5}) \end{aligned}$$

where the subscript i runs from A to B , and the factor \mathcal{N}_i has the following definition: $\mathcal{N}_A = 1$ and $\mathcal{N}_B = -1$. Here, we also have the following definitions:

$$A_{xyzw} = (1 - x - y - z - w), B_{xyz} = (1 - x - y - z), \quad (\text{A6})$$

$$H_{xyzw} = \left(\frac{1}{x} + \frac{1}{y} + \frac{1}{z} + \frac{1}{w} \right) m_c^2 - s, \quad (\text{A7})$$

$$F_{xyz} = \left(\frac{1}{x} + \frac{1}{y} + \frac{1}{z} + \frac{1}{1 - x - y - z} \right) m_c^2 - s, \quad (\text{A8})$$

$$x_{\pm} = \left[\left(1 - \frac{8m_c^2}{s} \right) \pm \sqrt{\left(1 - \frac{8m_c^2}{s} \right)^2 - \frac{4m_c^2}{s}} \right] / 2, \quad (\text{A9})$$

$$y_{\pm} = \left[1 + 2x + \frac{3sx^2}{m_c^2 - sx} \pm \sqrt{\frac{[m_c^2 + sx(x-1)][(8x+1)m_c^2 + sx(x-1)]}{(m_c^2 - sx)^2}} \right] / 2, \quad (\text{A10})$$

$$z_{\pm} = \left[(1 - x - y) \pm \sqrt{\frac{(x+y-1)[m_c^2(x+y-(x-y)^2) + sxy(x+y-1)]}{sxy - (x+y)m_c^2}} \right] / 2 \quad (\text{A11})$$

$$w_- = \frac{xyzm_c^2}{sxyz - (xy + yz + xz)m_c^2}, w_+ = 1 - x - y - z. \quad (\text{A12})$$

2. The spectral densities for 0^{-+} double hidden-charm hybrid

For all currents given in (3) and (4), we obtain the spectral densities as follows:

$$\begin{aligned} \rho_i^{\text{pert}}(s) &= \frac{g_s^2}{2^{10} \times 5 \times \pi^8} \int_{x_-}^{x_+} dx \int_{y_-}^{y_+} dy \int_{z_-}^{z_+} dz \int_{w_-}^{w_+} dw A_{xyzw} H_{xyzw}^3 \\ &\times \left\{ -4A_{xyzw} H_{xyzw}^3 xyzw + 2H_{xyzw}^2 [18xyzw A_{xyzw} s + \mathcal{N}_i (3A_{xyzw} - 1) \right. \\ &\times (xy + zw)m_c^2] + 20s A_{xyzw} (m_c^2 + \mathcal{N}_i xys)(m_c^2 + \mathcal{N}_i wzs) \\ &- 5H_{xyzw} [12xyzw A_{xyzw} s^2 + \mathcal{N}_i (6A_{xyzw} - 1)(xy + zw)m_c^2 s \\ &\left. + 2(A_{xyzw} - 1)m_c^4 \right\}, \quad (\text{A13}) \end{aligned}$$

$$\begin{aligned} \rho_i^{\langle G^2 \rangle}(s) &= \frac{\langle g_s^2 G^2 \rangle}{2^9 \times 3 \times \pi^6} \int_{x_-}^{x_+} dx \int_{y_-}^{y_+} dy \int_{z_-}^{z_+} dz F_{xyz}^2 \\ &\times \left\{ 6m_c^4 + \mathcal{N}_i m_c^2 (3s - 2F_{xyz})(xy + zB_{xyz}) \right\}, \quad (\text{A14}) \end{aligned}$$

$$\begin{aligned} \rho_i^{\langle G^3 \rangle}(s) &= \frac{\langle g_s^3 G^3 \rangle}{2^8 \times \pi^6} \int_{x_-}^{x_+} dx \int_{y_-}^{y_+} dy \int_{z_-}^{z_+} dz \left\{ -\frac{1}{2} [4xyz B_{xyz} F_{xyz}^3 \right. \\ &+ s(m_c^4 - s^2 xyz B_{xyz}) - 18F_{xyz}^2 sxyz B_{xyz} + 2F_{xyz} (6s^2 xyz B_{xyz} - m_c^4)] \\ &\left. + \frac{m_c^2 F_{xyz}}{x} [\mathcal{N}_i (F_{xyz} - s)(xy + zB_{xyz}) - 2m_c^2] \right\}. \quad (\text{A15}) \end{aligned}$$